Structural and Raman characterization of nanogranular BaTiO$_3$-NiFe$_2$O$_4$ thin films deposited by laser ablation on Si/Pt substrates

J.R. Gonçalves[1], J. Barbosa[1], P. Sá[1], J.A. Mendes[1,2], A.G. Rolo[1], B.G. Almeida[*,1]

[1] Departamento de Física, Universidade do Minho, Campus de Gualtar, 4710-057 Braga, Portugal
[2] ESEIG, IPP, Rua D. Sancho I, 981, 4480-876 Vila do Conde, Portugal

* Corresponding author: e-mail bernardo@fisica.uminho.pt, Phone: +351 253 604 063, Fax: +351 253

Thin films composed by (BaTiO$_3$)$_{1-x}$-(NiFe$_2$O$_4$)$_x$ with different nickel ferrite concentrations (*x*) have been deposited by pulsed laser ablation on platinum covered Si(001) substrates. The films structure was studied by X-ray diffraction and Raman spectroscopy. It was found that the NiFe$_2$O$_4$ phase unit cell was expanded along the growth direction of the films, with a lattice parameter that increased with increasing NiFe$_2$O$_4$ concentration. The opposite behavior was observed on the BaTiO$_3$ phase, with an expansion of its unit cell that lowered with increasing *x*. The presence of the strain in the films induced a redshift of the Raman peaks of NiFe$_2$O$_4$ that decreased with increasing NiFe$_2$O$_4$ concentration. Cation disorder in the nickel ferrite was observed for lower *x*, where the nanograins are more isolated and subjected to more strain, which was progressively decreased for higher NiFe$_2$O$_4$ content in the films.

1 Introduction The synthesis of multiferroic materials made by combining ferroelectric (piezoelectric) and ferromagnetic (magnetostrictive) substances has been attracting much scientific and technological interest [1-3]. In these composites, the elastic interaction between both phases induces a coupling between the magnetic and electric degrees of freedom, the so-called magnetoelectric effect. When a magnetic field is applied to the composite, the magnetic phase changes its shape magnetostrictively. Strain is then passed along to the piezoelectric phase, resulting in an electric polarization. For the converse effect a similar coupling is obtained.

Nanostructured multiferroic composites composed by barium titanate (BaTiO$_3$ – piezoelectric) and cobalt ferrite (CoFe$_2$O$_4$ –magnetostrictive) have been deposited by laser ablation, and magnetoelectricity has been demonstrated [2]. Nickel ferrite (NiFe$_2$O$_4$) is a good alternative to CoFe$_2$O$_4$ for the production of these nanostructured multiferroic composites. It has a simple structure, high electrical resistivity (~10^9 Ω cm) and relatively high magnetostriction [4,5]. Its Curie temperature is 585ºC [5].

As a result of the elastic interaction between the magnetostrictive and piezoelectric component phases, the properties and performance of the composite nanostructures depend critically on the phase morphology and internal stress distribution, which, in turn, are determined by the elastic phase/phase and phase/substrate interactions. In order to address this problem, nanogranular thin films composed by BaTiO$_3$ and NiFe$_2$O$_4$ (magnetostrictive), with different relative concentrations, were prepared by pulsed laser ablation on platinum covered Si(001) substrates.

NiFe$_2$O$_4$ has a cubic inverse spinel structure [4] in which eight Ni^{2+} ions occupy octahedral B sites along with an equal number of randomly distributed Fe^{3+} ions, whilst the remaining eight Fe^{3+} ions occupy the tetrahedral A sites.

Barium titanate is a well studied ferroelectric perovskite and is a good candidate for high-performance lead-free piezoelectric applications [4]. At high temperatures BaTiO$_3$ is cubic, in which the large barium ions are surrounded by twelve nearest-neighbor oxygens and each titanium ion has six oxygen ions in octahedral coordination. The barium and oxygen ions together form a face centered
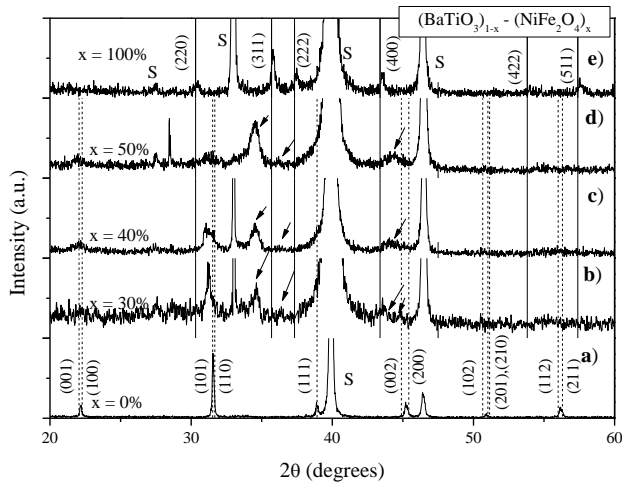
Figure 1 X-ray diffraction spectra of the samples deposited with nickel ferrite concentrations x = 0%, 30%, 40%, 50% and 100%. The vertical lines mark the peak positions of the bulk $NiFe_2O_4$ cubic spinel phase (——), and the tetragonal-$BaTiO_3$ phase (…).The peaks marked with an S are from the substrate.

cubic lattice, with titanium ions fitting in octahedral interstices. Below ~130 ºC $BaTiO_3$ transforms to a tetragonal structure, that remains at ambient temperature. The high temperature cubic phase is paraelectric and the ambient temperature tetragonal phase is ferroelectric.

2 Experimental details The $BaTiO_3$-$NiFe_2O_4$ thin films were prepared by laser ablation, on platinum covered Si(001) substrates. The depositions were done with a KrF excimer laser (wavelength λ = 248 nm), at a fluence of 2 J/cm². The pulse duration of the laser was 25 ns and the repetition rate was 10 Hz. The films were deposited in a reactive oxygen atmosphere, with an oxygen pressure of 1 mbar. The target to substrate distance was 5 cm and the substrate temperature was 650ºC.

The ablation targets were obtained by sintering $NiFe_2O_4$ and $BaTiO_3$ powders (with 1-2 μm average grain sizes) with nickel ferrite weight concentrations of x = 0% (pure $BaTiO_3$), 30%, 40%, 50% and 100% (pure $NiFe_2O_4$). Structural studies were performed by X-ray diffraction (XRD), using a Philips PW-1710 diffractometer with CuKα radiation. Raman studies were performed using a Jobin-Yvon T64000 spectrometer with an excitation wavelength at 514.5 nm, from an Ar laser.

3 Results and discussion Figure 1 shows the X-ray diffraction spectra measured on the nanocomposites with nickel ferrite concentrations in the range 30% - 50%. For comparison, the end members $BaTiO_3$ and $NiFe_2O_4$ are also shown. The films are polycrystalline and composed by a mixture of tetragonal-$BaTiO_3$ and $NiFe_2O_4$ with cubic inverse spinel structure [6]. As the concentration of the nickel ferrite increases the relative intensity of the (311) $NiFe_2O_4$ peak increases, indicating the progressively more oriented growth of this phase. On the composites, an over-
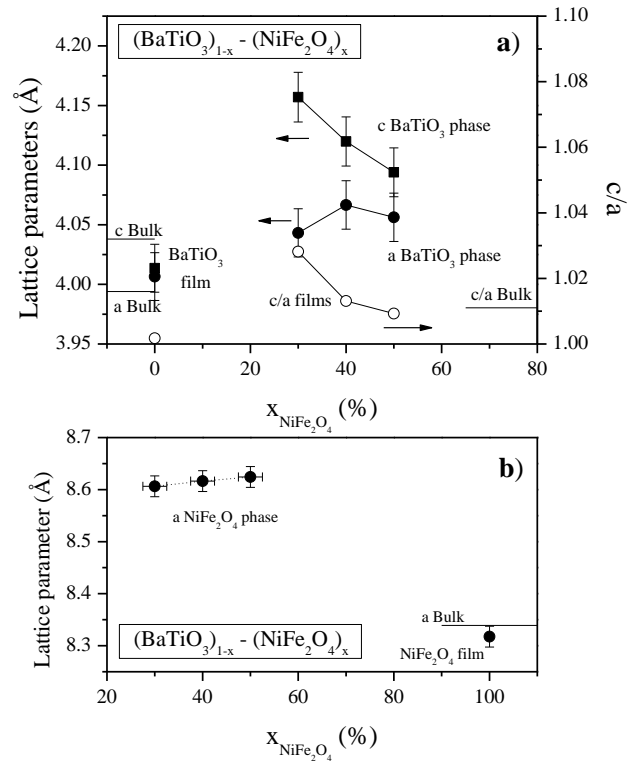

Figure 2 Lattice parameters a) *a* and *c* (left axis) of the tetragonal-$BaTiO_3$ component phase and b) of the $NiFe_2O_4$ component phase on the nanocomposites. The values were obtained from the (200) and (002) peak positions of $BaTiO_3$, and from the (311) peak position of $NiFe_2O_4$. On the right axis of a) is the c/a ratio of the $BaTiO_3$ phase for the same samples.

all shift of the diffraction peaks to lower angles is observed, as compared with their corresponding reference values (fig. 1). As such,, the peaks were fitted using pseudo-Voigt functions in order to determine their angular positions and integral widths. The grain sizes obtained from the fitted X-ray diffraction peak widths for both phases (from the (311) peak for $NiFe_2O_4$ and the (002) peak for $BaTiO_3$), were determined by using the Scherrer equation [7]. They are in the range 20 - 71 nm for the barium titanate phase and 15 - 22 nm for the $NiFe_2O_4$ one.

Figure 2a) (left axis) shows the lattice parameters of the barium titanate phase determined from the fitted (002) and (200) peak positions. On the right axis of the figure the ratio between the *c* and *a* lattice parameters is represented. For the pure barium titanate film, *a* is slightly expanded and *c* is slightly contracted related to the bulk, giving a lower tetragonal distortion of the $BaTiO_3$ structure as indicated by a lower c/a ratio. On the other hand, on studied the $BaTiO_3$-$NiFe_2O_4$ composites, the *a* and *c* lattice parameters of the $BaTiO_3$ phase are always above the bulk ones, decreasing with increasing nickel ferrite concentration up to x = 50%. However, their c/a ratio keeps near from the bulk one, indication and overall expansion of the unit cell

that is decreasing with increasing $NiFe_2O_4$ content (up to $x = 50\%$).

On the other hand, the lattice parameter of the $NiFe_2O_4$ phase, obtained from the (311) peak position (figure 2b), is always above the bulk value ($a_{bulk} = 4.339$Å) and varies from 8.606 Å on the sample with lower nickel ferrite concentration ($x=30\%$), to 8.624 Å on the sample with higher $NiFe_2O_4$ content ($x=50\%$). Comparing with the bulk $NiFe_2O_4$, in the films the nickel ferrite unit cell has an expansion strain that increases as its concentration increases, up to x=50%. Since the lattice parameter was determined from θ-2θ measurements (spectra of figure 1), which scan the films structure in the direction perpendicular to their surface, this indicates that the lattice planes are expanded along the growth direction of these films.

Figure 3 shows the Raman spectra of the thin film samples deposited with nickel ferrite concentrations in the range 30%-50%. Also shown are the individual $BaTiO_3$ and $NiFe_2O_4$ bulk reference powders, for comparison.

On the films, several bands of the $NiFe_2O_4$ phase are observed on the spectra and their positions are represented by solid lines in figure 3. Two of them are more clearly visible and they appear near 570 cm^{-1} and 700 cm^{-1}. In the $BaTiO_3$ case, the bands are more difficult to observe since they are superimposed with the ones of $NiFe_2O_4$, particularly in the wavenumber ranges of 250-350 cm^{-1} and 450-550 cm^{-1}. Nevertheless, the peak at 716 cm^{-1}, corresponding to the longitudinal optical (LO) vibration of the E phonon mode [8], can be followed in the different nanocomposites and the decrease of its intensity with increasing nickel ferrite concentration reflects the corresponding decrease of the barium titanate content in the films. This Raman E peak at 716 cm^{-1} is characteristic of the $BaTiO_3$ tetragonal (ferroelectric) structure [9] and indicates its presence on the barium titanate phase of the deposited composite films.

The spinel ferrite structure AFe_2O_4 has the space group Fd3m (O_g^7) and factor group analysis predicts five Raman active modes, namely, two A_{1g}, two E_g and one T_{2g} modes [10]. The inverse spinel structure of AFe_2O_4 consists of AO_6 and FeO_4 octahedra and FeO_6 tetrahedra. The modes arising from the octahedra and tetrahedra can be easily distinguished in the Raman spectrum of ferrites. Raman peaks over the region 660-720 cm^{-1} represent the modes of tetrahedra and those in 460-660 cm^{-1} region correspond to modes of octahedra [10]. Then, the nickel ferrite modes appearing at 570 cm^{-1} and 700 cm^{-1} can then be assigned to octahedral site (O-site) sublattice and tetrahedral site (T-site) sublattice vibration modes, respectively [10]. They reflect the local lattice effects in the tetrahedral and octahedral sublattices.

Based on the peaks observed on the powders, the nanocomposite films spectra were deconvoluted by using Lorentzian line-shape functions to least-squares fit the Raman peaks. Figure 3 shows the fitted lorentzians for the particular case where the concentration of the nickel ferrite is $x = 40\%$. From the fitted lorentzians, the vibrational modes wavenumber was determined by the peak position.
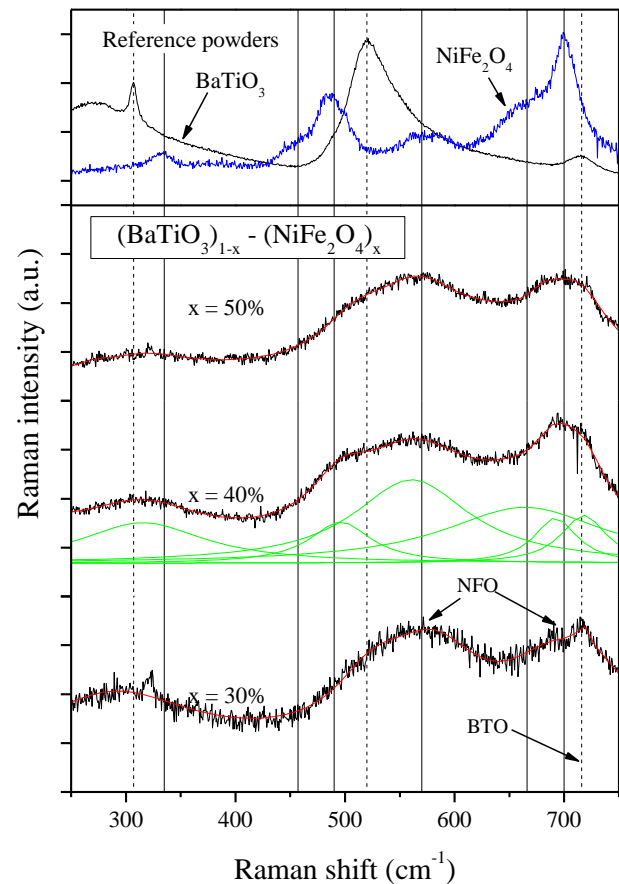

Figure 3 Raman spectra of the samples deposited with $NiFe_2O_4$ concentrations of 30%, 40% and 50%. Also shown are the $BaTiO_3$ and $NiFe_2O_4$ reference powders and the Lorentzians obtained from the fit to the spectrum of the sample with x = 40%.
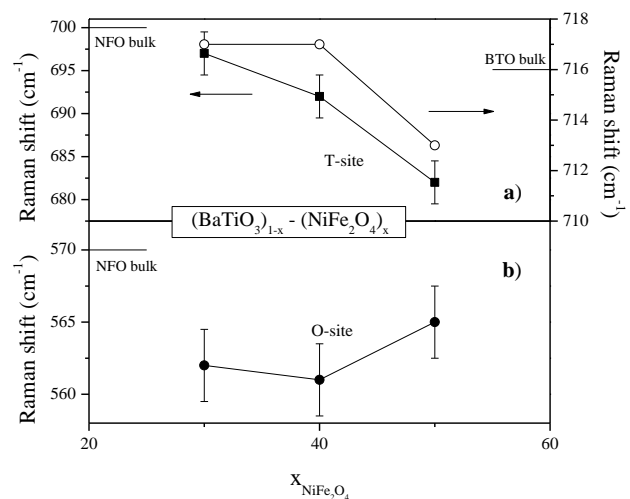

Figure 4 Raman shift as a function of the $NiFe_2O_4$ concentration, for the a) left: T-site and b) O-site modes. On the right axis of a) is the E(LO) mode of $BaTiO_3$ which appears at 716 cm^{-1} in the bulk. The error bars on the E mode are similar to the ones of the T-site mode of $NiFe_2O_4$.
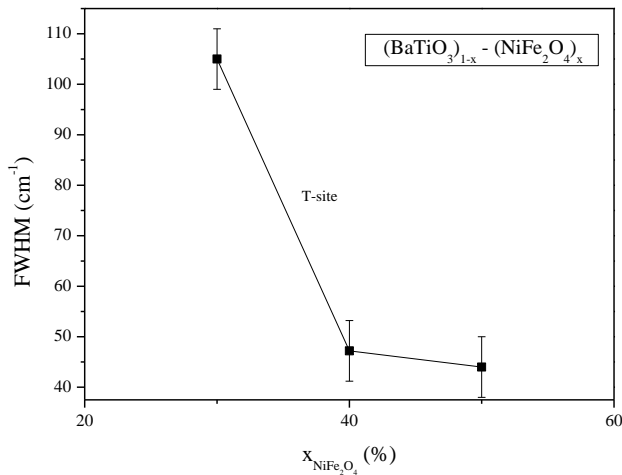
Figure 5 Full wide half maximum (FWHM) of the fitted lorentzians as a function of the NiFe$_2$O$_4$ concentration, for the T-site mode.

Figure 4 shows the wavenumbers for the O-site and T-site Raman peaks of the NiFe$_2$O$_4$ phase as well as the BaTiO$_3$ phase E(LO) peak near 716 cm^{-1}. As the nickel ferrite concentration increases, the barium titanate E(LO) peak of figure 4 is near and somewhat oscillates around the bulk value. On the other hand, the NiFe$_2$O$_4$ T-site mode has a redshift on the nanocomposites, with its wavenumber being systematically below the bulk value. A similar trend is observed for the O-site mode. This redshift of the NiFe$_2$O$_4$ modes results from the expansion of the lattice parameter of the nickel ferrite, as was similarly observed from the X-ray diffraction results (fig. 1 and fig. 2).

The full-wide-at-half-maximum (FWHM, damping factor) for the T-site mode peak of the nickel ferrite phase is shown in figure 5. A decrease of FWHM with increasing NiFe$_2$O$_4$ concentration is observed on the nanocomposites. This decrease can be attributed to the decrease of cation disorder in the films [11]. In fact, the results shown in figure 5 indicate that NiFe$_2$O$_4$ nanoparticles are more disordered at lower concentrations. As the NiFe$_2$O$_4$ content in the films is increased, more nickel ferrite nanograins become connected, cation disorder is reduced, so that at higher NiFe$_2$O$_4$ concentrations a decreased value of damping factor is obtained.

4 Conclusions Nanocomposites of nickel ferrite grains mixed in a barium titanate matrix were deposited by pulsed laser ablation, with different NiFe$_2$O$_4$ concentrations. The nickel ferrite nanograins were under expansion strain that increased with increasing NiFe$_2$O$_4$ concentration, on the prepared concentration range. Due to this, the Raman lines of the NiFe$_2$O$_4$ phase presented a corresponding redshift on their wavenumbers. Disorder of the cation distribution in the nickel ferrite was observed for lower NiFe$_2$O$_4$ concentration that was decreased for higher NiFe$_2$O$_4$ content in the films.

References

[1] W. Eerenstein, N. D. Mathur, J. F. Scott, Nature, **442**, 759 (2006).
[2] R. Ramesh and N. A. Spaldin, Nature Mat., 6, 21 (2007).
[3] Ce-Wen Nan, M.I. Bichurin, Shuxiang Dong, D. Viehland, G. Srinivasan, J. App. Phys., **103**, 031101 (2008).
[4] A.J. Moulson, J.M. Herbert, "Electroceramics", (Chapman and Hall, London, 1997), p. 68-79 and 387-389.
[5] S. Chikazumi, "Physics of Ferromagnetism", (Oxford University Press, New York, 1997), p. 199-201.
[6] Powder Diffraction File, Joint Committee on Powder Diffraction Standards, International Centre for Diffraction Data, Cards 10-325 and 5-626, (2004)
[7] B.D. Cullity, S.R. Stock, "Elements of X-Ray Diffraction", (Prentice Hall, New Jersey, 2001).
[8] U.V. Venkateswaran, V.M. Naik and R. Naik, Phys. Rev. B, **58**, 14256 (1999).
[9] Y. Shiratori, C. Pithan, J. Dornseiffer, R. Waser, J. Raman Spectrosc., 38, 1300 (2007)
[10] S.P. Sanyal, R.K. Singh, "Phonons in condensed materials", (Allied Publishers, New Delhi, 2004), p. 164.
[11] Z. H. Zhou, J. M. Xue, J. Wanga, H. S. O. Chan, T. Yu, Z. X. Shen, J. Appl. Phys., **91**, 6015 (2002)